

## **2. Objectives and experimental work**

The contemporary research focuses on catalytic driven industrial production which makes the environment less polluting<sup>1-4</sup>. Transition metal complexes are one of the most valuable and potent catalysts for industrial processes. However, these traditional homogeneous catalysts are hampering from various complexities despite excellent catalytic function<sup>5-10</sup>. For this reason, catalysis research mainly focuses on the development of the catalysts that can function with better atom economy, simplest and greener procedure and last longer and hence the centre of attention for advanced research is the development of solid-supported heterogeneous catalysts as another possibility<sup>11-22</sup>. Amongst all the available solid supports, graphite and graphene oxide have fascinated enormous attention as an emerging support material for fundamental science and applied research owing to its extraordinary properties<sup>23-29</sup>. A major problem in graphene study is the bulk production of graphene sheets. Besides the first attempt of Brodie<sup>30</sup> in 1859 to produce single graphene sheet by exfoliation, a numerous attempts had been made by other researchers but the massive production of single graphene sheet has not been procured so far<sup>31-35</sup>.

Graphene can be synthesized by mechanical cleavage, thermal exfoliation, and chemical functionalization<sup>33,36</sup>. Amongst them, chemical functionalization is promising and simplest route that functionalize the carbon backbone. Creating defect in the carbon backbone is the promising practice which can effectively trap the diffusing atoms and group. Graphene oxide (GO) contains such defects throughout the scaffold which accommodate vacancies, hole defect and oxidative functional groups for example carboxyl, epoxy and hydroxyl groups<sup>37-39</sup> on both side of the sheet on its basal plane and edges that can act as nucleation centres and anchoring sites for atoms or groups other than carbon<sup>40,41</sup>. However, if pristine GO is used for the selective oxidation reactions, for instance, selective oxidation of benzyl alcohol, the eliminating hydrogen atoms from the organic molecules converts the epoxy groups adorning the basal plane of GO to the diol groups by ring opening. This progression of formation of diol on the surface of GO increases the C:O ratio which significantly inhibits the selective oxidation reaction and decrease

the yield due to considerable reduction in the number of catalytic active sites in the vicinity of reaction<sup>42</sup>.

Hence, these functional groups were selectively functionalized by appropriate organic and/or inorganic moiety. For example, hydroxyl groups can effectively be modified by amino groups; however, carboxyl groups can successfully be activated by thionyl groups. Z. Li et al.<sup>43</sup> have synthesized graphene oxide supported heterogeneous catalysts by modifying the surface hydroxyl groups using APTES followed by grafting of CM–Salen H<sub>2</sub> metal complexes. The heterogenized cobalt and copper complexes (Co/Cu–Salen–GO) were inspected over the epoxidation of styrene using air as an oxidant. Q. Zhao and his co-workers<sup>44</sup> covalently modified GO using 3-aminopropyltrimethoxysilane (APTMS) followed by condensation with salicylaldehyde. The copper complex was then grafted on this salen modified GO which formed tetrahedral chelate structure [Cu(salen)-*f*-GO]. They used this heterogeneous catalyst for the epoxidation of olefins using TBHP as an oxidant. Graphene oxide immobilized Cu(II) Schiff base complex (GO@AF-SB-Cu), was prepared by the reaction of a Schiff base functionalized GO by A. Kumar et al.<sup>45</sup>. The catalytic activity of the as-synthesized compound was examined over Chan-Lam coupling reaction of amines and phenylboronic acid. Functionalization at carboxylic acid groups was exhibited by S. Niyogi and his group<sup>46</sup>. They refluxed 100 mg GO in 20 mL of SOCl<sub>2</sub> in presence of 0.5 mL of DMF at 70 °C for 24 h. This chloro functionalized GO sheet was allowed to react with octadecylamine and the yield of the reaction was 20 wt% of oxidized graphite. Y. Xu et al.<sup>47</sup> had refluxed 30 mg of GO in 20 mL of SOCl<sub>2</sub> in presence of 0.5 mL of DMF at 70 °C for 24 h. It was then further reacted with TPP-NH<sub>2</sub> in DMF in the presence of Et<sub>3</sub>N and the product was subjected to nylon membrane filtration and re-suspension in THF to produce TPP-NHCO-SPFGraphen. GO sheet was refluxed with SOCl<sub>2</sub> at 70 °C for 24 h by Z. B. Liu and his group<sup>48,49</sup> to synthesize graphene nanohybrid with porphyrin and fullerene, respectively. In this reaction, graphene sheet was combined with porphyrin and fullerene through mild coupling reaction of the –COOH group of GO with –NH<sub>2</sub> group of porphyrin and –OH group of pyrrolidine fullerene.

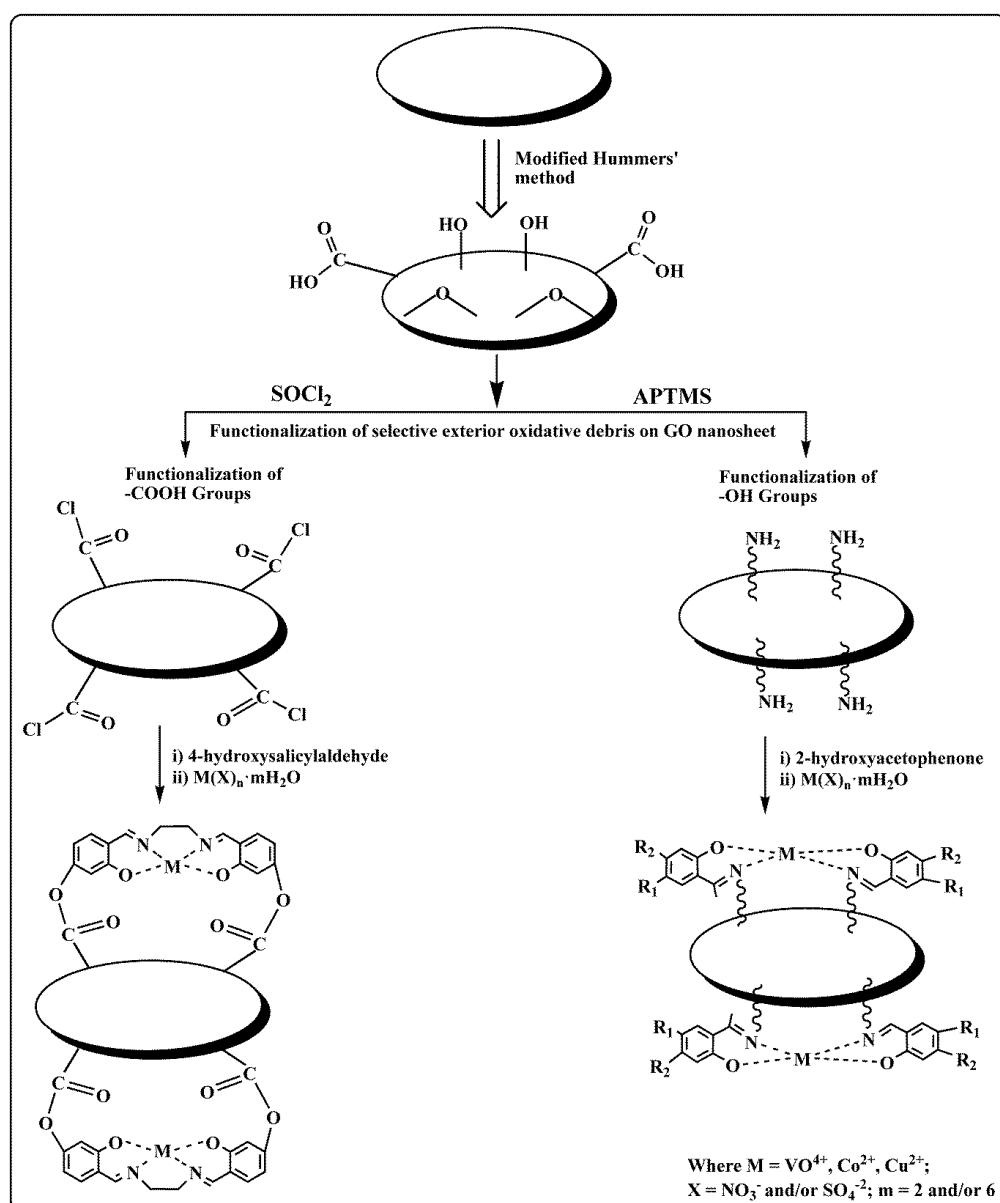
After the successful modification of oxygenated functional groups, grafting of metal or metal salen complex was executed for the desired sturdy and lasting heterogeneous catalysts. However, in catalysis, ligands with number of donor sites play a crucial role<sup>50-52</sup> as it can tune the properties of metal ion/ complexes and consequently its reactivity and applications. Therefore, one needs to be more careful in choosing and grafting of proper ligand.

In this chapter, we have fabricated GO supported transition metal complexes via ligand spacer as heterogeneous catalysts. In sequential synthesis, graphite flakes were oxidized using modified Hummers' method<sup>53</sup> to produce GO. This as-prepared GO nanosheet was used to fabricate the as-stated heterogeneous catalysts. Amongst the available methods for covalent attachment of metal/ metal complexes onto the graphene nanosheet, we have chosen the grafting method. The hydroxyl groups were selectively functionalized by using APTMS followed by grafting with Schiff base ligand such as 2-hydroxyacetophenone (2-AcPh) and different transition metals viz.  $\text{Cu}(\text{NO}_3)_2 \cdot 6\text{H}_2\text{O}$ ,  $\text{VOSO}_4 \cdot 2\text{H}_2\text{O}$  and  $\text{Co}(\text{NO}_3)_2 \cdot 6\text{H}_2\text{O}$ . On the other hand, carboxyl groups were selectively modified by thionyl chloride ( $\text{SOCl}_2$ ) in the first step. While in the second step, salen ligand was prepared from 4-hydroxysalicylaldehyde and ethylenediamine. This salen ligand was then treated with different metal salts like  $\text{Cu}(\text{NO}_3)_2 \cdot 6\text{H}_2\text{O}$ ,  $\text{VOSO}_4 \cdot 2\text{H}_2\text{O}$  and  $\text{Co}(\text{NO}_3)_2 \cdot 6\text{H}_2\text{O}$  to form metal-salen complex. In the final step, chloro modified GO nanosheet (Cl-*f*-GO) was treated with metal-salen complexes  $[\text{M}(\text{L})_n]$  to fabricate the desired heterogeneous catalysts  $[\text{M}(\text{L})_n\text{-}f\text{-GO}]$  as screened in Scheme 2.1. The as-prepared heterogeneous catalysts were evaluated against the catalytic oxidation of benzyl alcohol, glucose, epoxidation of styrene and norbornene through optimization of various parameters like mole ratio of substrate to oxidant, catalyst amount, temperature, time, solvents, amount of solvent, varying oxidants etc.

## **2.1. Objectives**

Based on the above rationalization we have sketched out the roadmap to perform the research work with the following **main objectives**:

- ❖ Synthesis and characterization of graphene oxide (GO) and functionalized GO (*f*-GO) nanosheets.
- ❖ Synthesis and characterization of covalent tethering of transition metal complexes on *f*-GO [ $M(L)_n$ -*f*-GO].
- ❖ To study the catalytic competence of synthesized catalysts over possible diverse catalytic reactions.
- ❖ Optimal catalyst will be developed and chosen for scale-up reactions.



**Scheme 2.1.** General scheme for the synthesis of catalysts by functionalization of -OH and -COOH groups of GO.

## 2.2. Experimental

### 2.2.1. Materials and methods

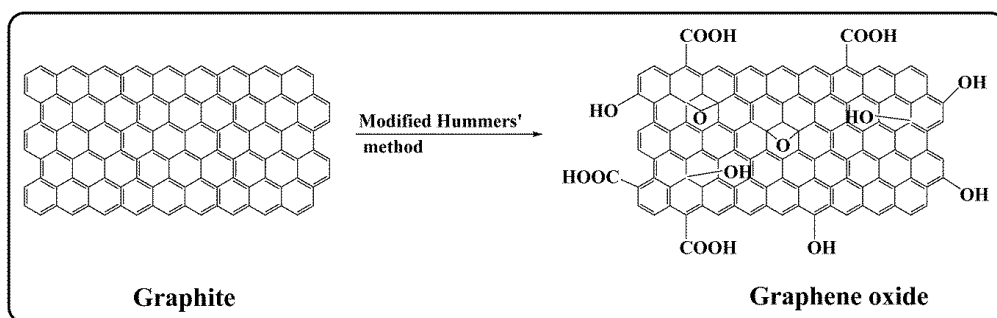
Natural flake graphite (325 mesh, 99.95%) was purchased from Sigma Aldrich, conc. sulphuric acid ( $\text{H}_2\text{SO}_4$ , 98%), conc. nitric acid ( $\text{HNO}_3$ ), sodium nitrate ( $\text{NaNO}_3$ ), conc. hydrochloric acid ( $\text{HCl}$ , 35-38%), hydrogen peroxide (30%,  $\text{H}_2\text{O}_2$ ), tert-butyl hydroperoxide (TBHP), metal salts such as  $\text{Cu}(\text{NO}_3)_2 \cdot 6\text{H}_2\text{O}$ ,  $\text{VOSO}_4 \cdot 2\text{H}_2\text{O}$ ,  $\text{Co}(\text{NO}_3)_2 \cdot 6\text{H}_2\text{O}$ , reagents like thionyl chloride ( $\text{SOCl}_2$ ), ethylenediamine, sodium acetate ( $\text{CH}_3\text{COONa}$ ), 4-hydroxysalicylaldehyde, benzyl alcohol, benzaldehyde, benzoic acid, styrene monomer, styrene oxide, phenyl acetaldehyde, norbornene, norbornene oxide and gluconic acid, solvents such as methanol, dimethylformamide (DMF), toluene, 1,4-dioxane, acetonitrile, ethylene glycol, were purchased from S D Fine Chem Ltd. Potassium permanganate ( $\text{KMnO}_4$ ) was purchased from E. Merck India Pvt. Ltd. 3-aminopropyltrimethoxysilane (APTMS) was purchased from Alfa Aesar, graphite flakes (60 mesh size), 2-hydroxycetophenone and glucose was purchased from Chemdyes Corporation, Rajkot. All the chemicals and reagents were of analytical grade and used as received without further purification for the material synthesis.

### 2.2.2. Synthesis of graphene oxide (GO)

GO was synthesized from natural flake graphite using modified Hummers' method<sup>54</sup> (Scheme 2.2). This method includes both the oxidation and exfoliation of graphite sheet as it incorporates the sonication and thermal treatment. The step wise synthesis of GO is given as follows:

2000 mg of graphite flakes and 2000 mg of  $\text{NaNO}_3$  were stirred in 90 mL of 98%  $\text{H}_2\text{SO}_4$  in a 1000 mL volumetric flask which was kept in an ice bath to maintain the temperature between 0-5 °C followed by the addition of 1200 mg of  $\text{KMnO}_4$ . At this step, the rate of the addition of  $\text{KMnO}_4$  must be very slow to maintain the reaction temperature below 15 °C and the suspension was continued to stir for 6 h. After 4 h, 184 mL of deionised water was added very slowly and the mixture was allowed to stir for 2 h in an ice bath. The ice bath was then removed and the mixture was stirred for another 2 h at 35 °C followed by refluxing at 98 °C for 10-15 min and the temperature

was then changed to 30 °C which gives brown coloured solution. After 10 min of stirring, lowered the temperature to 25 °C and maintained for 2 h with continuous stirring. Afterwards, the solution was oxidized with 40 mL of 30% H<sub>2</sub>O<sub>2</sub> changing the colour of the solution from brown to bright yellow. This solution was divided in to two equal amounts and poured to two separate beakers filled with 200 mL of deionised water and stirred for 1 h. This mixture was then kept undisturbed for 6-8 h to allow the particle to settle down at the bottom and the supernatant water was allowed to filter out. The resulting mixture was then repetitively treated with 10% HCl by centrifugation and then washed with deionised water until pH becomes neutral. This gel like substance was dried in an oven at 80 °C until it becomes a hard film (Fig. 2.1) and crushed to obtain fine GO powder. The yield of GO was ~4000 mg.



**Scheme 2.2.** Synthesis of GO by modified Hummers' method.

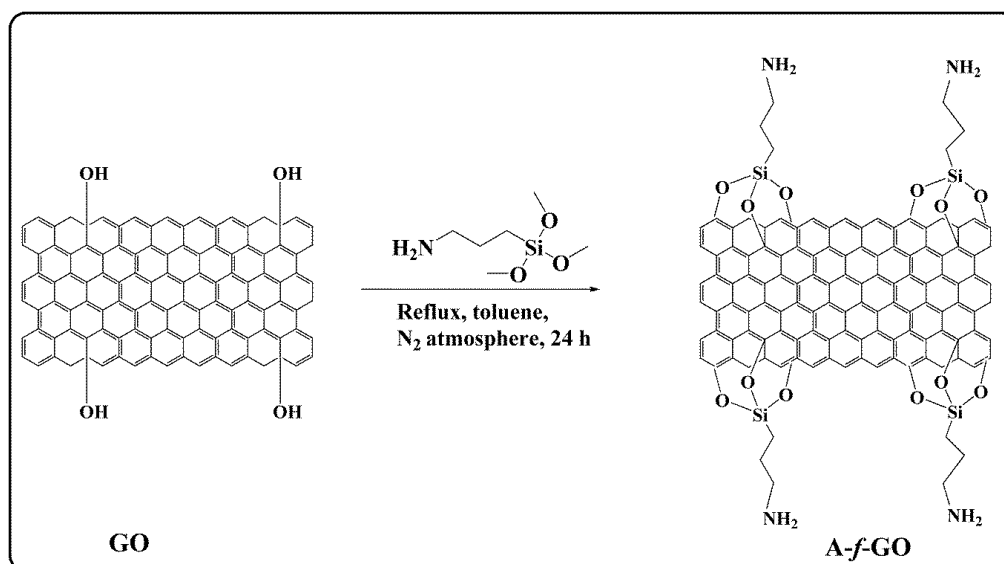


**Fig. 2.1.** An image of synthesized GO nanosheet and solution of GO.

### 2.2.3. Functionalization at –OH groups

#### 2.2.3.1. Preparation of amino functionalized GO (A-f-GO)

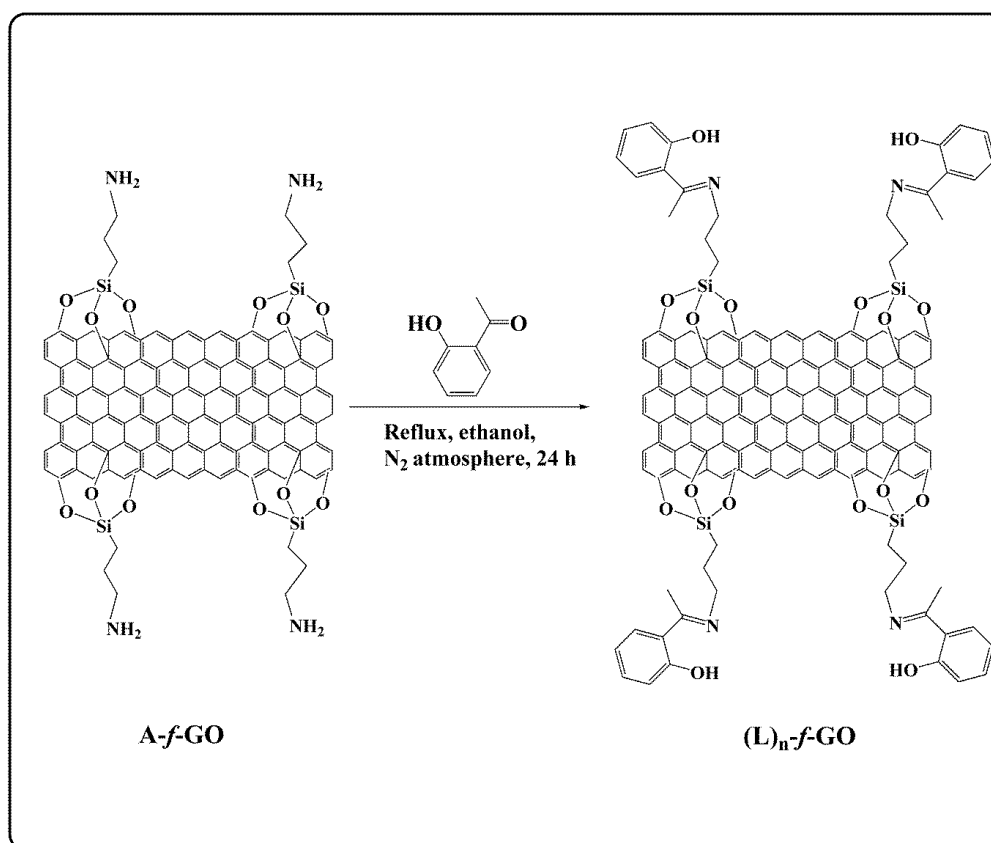
To functionalize the hydroxyl groups of GO nanosheet, it was treated with APTMS (Scheme 2.3). Dispersion of 1200 mg of GO in 250 mL of toluene was ultrasonicated for 45 min. This suspension was refluxed with 3.6 mL of APTMS at 110 °C for 24 h under N<sub>2</sub> atmosphere. The resulting mixture was filtered and washed with toluene repeatedly to remove un-reacted APTMS. After the successful functionalization, –NH<sub>2</sub> groups were served in place of hydroxyl groups presented on the surface of GO and obtained black solid was dried overnight in an oven at 110 °C. The yield of A-f-GO was observed ~1190 mg.



**Scheme 2.3.** Functionalization of hydroxyl groups.

#### 2.2.3.2. Preparation of Schiff base ligand functionalized GO [(L)<sub>n</sub>-f-GO]

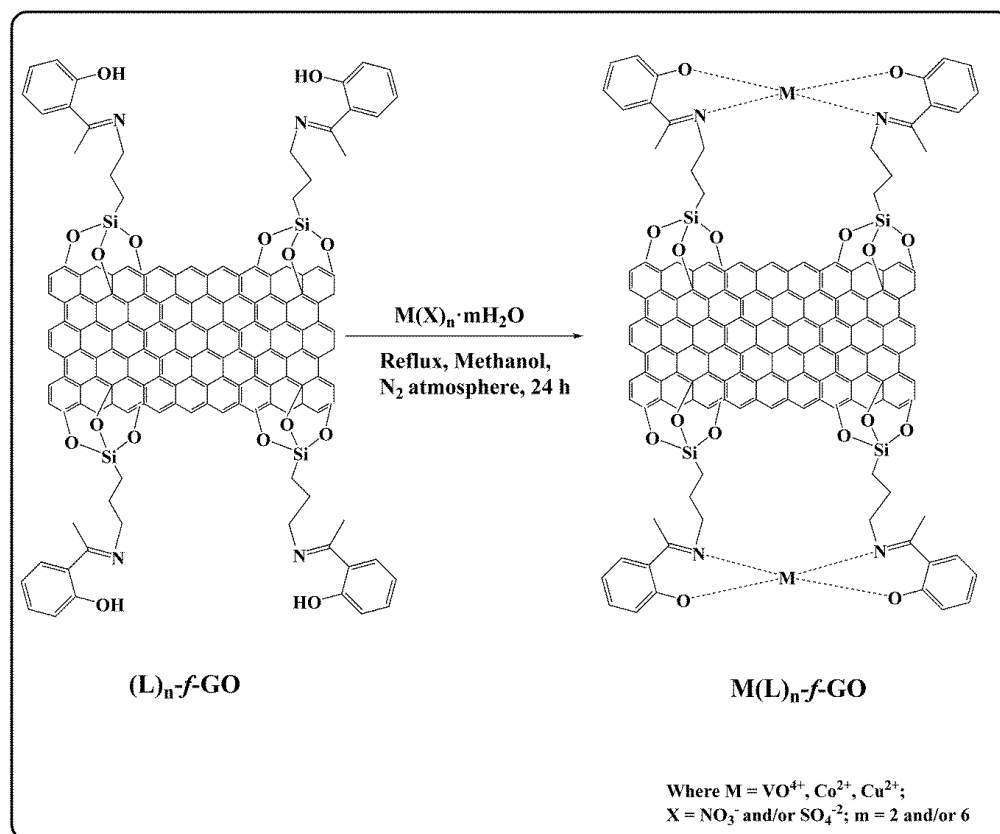
1000 mg of as-prepared A-f-GO was suspended in 150 mL of ethanol using ultrasonic bath for 45 min. The suspension was then refluxed with 2.4 mL of 2-hydroxyacetophenone at 80 °C for 8 h under N<sub>2</sub> atmosphere. After completion of the reaction, the obtained black solid product was washed with methanol several times and dried in an oven at 60 °C for 6 h. The yield of (L)<sub>n</sub>-f-GO (Scheme 2.4) obtained was ~1000 mg.



**Scheme 2.4.** Modification of A-f-GO with Schiff base ligand.

### 2.2.3.3. Preparation of catalysts [M(L)<sub>n</sub>-f-GO]

As-prepared 1000 mg of (L)<sub>n</sub>-f-GO was suspended in 150 mL of methanol using ultrasonic bath for 45 min. The suspension was then refluxed with 2000 mg of metal salts, for instance, Cu(NO<sub>3</sub>)<sub>2</sub>•6H<sub>2</sub>O, VOSO<sub>4</sub>•2H<sub>2</sub>O and Co(NO<sub>3</sub>)<sub>2</sub>•6H<sub>2</sub>O at 60 °C for 24 h under N<sub>2</sub> atmosphere. After completion of the reaction, the resulting mixture was filtered and repeatedly washed with methanol to remove un-reacted metal salts and then dried in an oven at 60 °C for 6 h to get black solid of the final catalysts (Scheme 2.5). The yield of M(L)<sub>n</sub>-f-GO obtained was ~1020 mg.

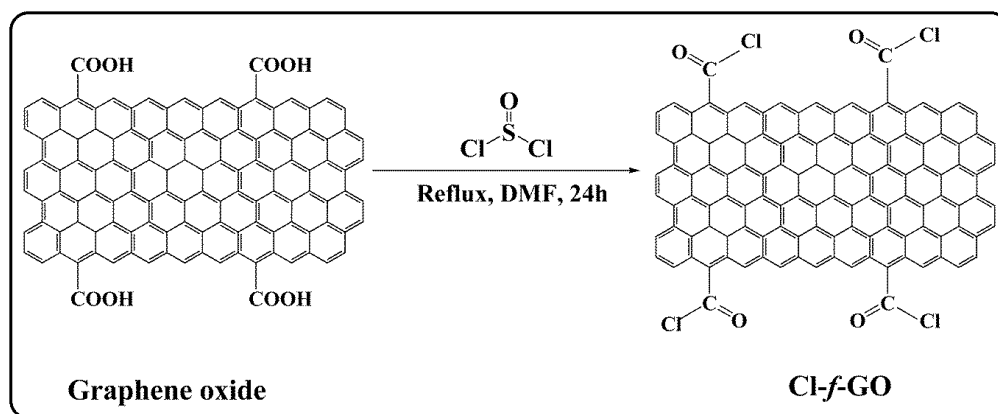


**Scheme 2.5.** Grafting of metal complex.

## 2.2.4. Functionalization at –COOH groups

### 2.2.4.1. Preparation of chloro functionalized GO (Cl-f-GO)

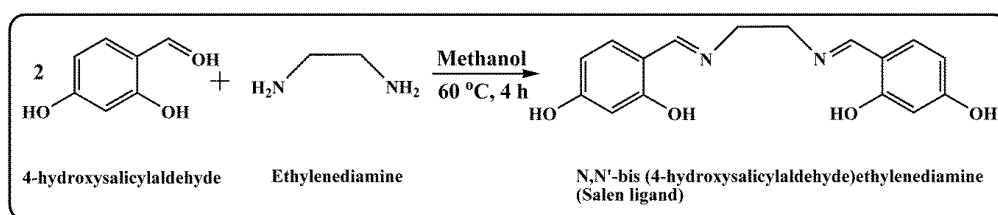
To initiate the functionalization at carboxyl groups, GO nanosheet was treated with thionyl chloride. 1000 mg of GO nanosheet was suspended in 10 mL of DMF followed by refluxing with 60 mL of thionyl chloride at 70 °C for 24 h using a  $CaCl_2$  guard tube. This reaction does not require  $N_2$  atmosphere. After completion of the reaction, excess thionyl chloride was removed from the reaction mixture by washing with toluene and methanol followed by drying in an oven at 80 °C for 8-12 h (Scheme 2.6). The obtained yield of Cl-f-GO was ~1040 mg.



**Scheme 2.6.** Functionalization of carboxyl groups.

#### 2.2.4.2. Preparation of salen ligand [H<sub>2</sub>L]

Salen refers to a tetra dentate C<sub>2</sub>-Symmetric ligand which easily coordinates the central metal ion and this metal-salen complex serves as a good catalyst. This salen ligand was synthesized by condensation reaction between 1400 mg of 4-hydroxysalicylaldehyde and 0.3 mL of ethylenediamine in methanol in 2:1 ratio at 60 °C for 4 h. This reaction does not require N<sub>2</sub> atmosphere. After completion of the reaction, the final yellow-brownish product was dried in an oven at 60 °C for 6 h to obtain salen ligand [N,N'-bis(4-hydroxysalicylaldehyde)ethylenediamine] (Scheme 2.7). The color of the final reaction mixture was yellow-brownish and the yield of salen ligand obtained was ~1000 mg.

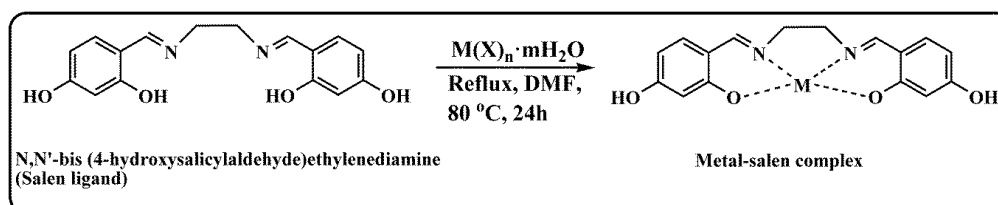


**Scheme 2.7.** Synthesis of salen ligand.

#### 2.2.4.3. Preparation of metal-salen complex

In the preparation of catalyst, moving one more step ahead, the as-prepared 600 mg of salen ligand was dissolved in 10 mL DMF and 600 mg of metal salts, for instance, Cu(NO<sub>3</sub>)<sub>2</sub>•6H<sub>2</sub>O, VOSO<sub>4</sub>•2H<sub>2</sub>O and Co(NO<sub>3</sub>)<sub>2</sub>•6H<sub>2</sub>O (in 1:1 mole ratio) was added followed by refluxing at 80 °C for 6 h. During

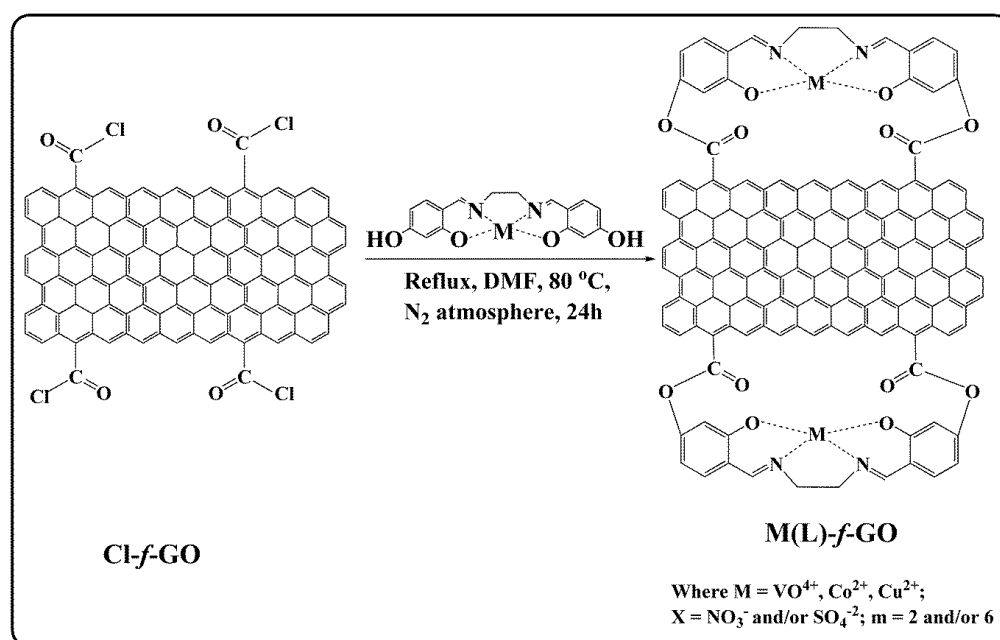
the preparation of metal-salen complex, sodium acetate was added to the reaction mixture to maintain the pH of the reaction mixture 5 to 6. The color of the reaction mixture was changed to reddish-brown. The resultant reaction mixture was filtered and dried in an oven to obtain ~1000 mg metal-salen complex (Scheme 2.8).



**Scheme 2.8.** Synthesis of metal-salen complex.

#### 2.2.4.4. Preparation of catalysts [M(L)-f-GO]

In this final step of preparation catalysts, the as-prepared 1000 mg of Cl-f-GO was dissolved in 5 mL of DMF and the solution of as-prepared metal-salen complex prepared by dissolving 1000 mg of metal-salen complex in 5 mL of DMF was mixed with it. This reaction mixture was then refluxed at 70 °C for 24 h under N<sub>2</sub> atmosphere (Scheme 2.9). After completion of the reaction, the excess amount of solvent was subjected to remove by evaporation at room temperature. The obtained black product was then dried in vacuum oven overnight to acquire the absolute heterogeneous catalysts. The obtained yield of M(L)-f-GO was ~1400 mg.



**Scheme 2.9.** Grafting of metal-salen complex onto Cl-f-GO.

### 2.3. Physico-chemical techniques

Chemical analysis is referred to as the qualitative and/or quantitative determination, identification and verification of materials which plays a crucial role probing and measuring the material's structure. It is a primary process in the field of materials science, without which no scientific insight of engineering materials could be ensured.

#### 2.3.1. Inductively coupled plasma optical emission spectroscopy (ICP-OES)

The quantitative analysis of transition metal ions in all the synthesized catalysts and silicon in the amino functionalized GO (A-f-GO) was performed by Inductive coupled plasma optical emission spectroscopy (ICP-OES) using ARCOS, Simultaneous ICP Spectrometer at SAIF, IIT, Bombay (Fig. 2.2). To estimate the percentage /ppm quantity of the metal ions and silicon in the samples, the solution was prepared by dissolving known quantity (10 mg) in aqua regia ( $\text{HCl} + \text{HNO}_3$  in 3:1 ratio). This solution was then diluted 10 times with deionised water.

This is the most common technique to choose a single wavelength for a given element. The intensity of the energy emitted at the selected wavelength

is proportional to the concentration of the respective element in the sample which is being analyzed. Hence, by determining the wavelengths emitted and their intensities, one can qualitatively and quantitatively find the elements from the given sample relative to a reference standard.



**Fig. 2.2.** Inductive coupled plasma atomic emission spectroscopy.

### **2.3.2. BET surface area and pore volume analyses**

BET theory is an extension of the Langmuir theory of monolayer molecular adsorption to multilayer adsorption the hypotheses given below:

- Gas molecules adsorb physically on a solid surface.
- Gas molecules act reciprocally with only adjacent layers.
- The Langmuir theory can be relevant to a piece layer.
- The enthalpy of adsorption for the first layer is constant and larger than the subsequent next layer.
- The enthalpy of adsorption for the second and higher subsequent layers is the same as the enthalpy of liquefaction.

The resulting BET equation is

$$\frac{1}{w[(p_o/p) - 1]} = \frac{c - 1}{w_m C} \left( \frac{p}{p_o} \right) + \frac{1}{w_m C}$$

Where  $p$  and  $p_0$  are the equilibrium and the saturation pressure of adsorbates at the temperature of adsorption,  $w$  is the adsorbed gas quantity, and  $w_m$  is the monolayer adsorbed gas quantity.  $C$  is the BET constant,

$$C = \exp\left(\frac{E_1 - E_L}{RT}\right)$$

Where  $E_1$  is the heat of adsorption for the first layer and  $E_L$  is for the second and higher layers and is equal to the heat of liquefaction or heat of vaporisation.

BET (Brunauer, Emmett and Teller) surface area and pore volume of the synthesized catalysts [M(L)<sub>n</sub>-f-GO] were measured by multipoint BET method using Micromeritics ASAP 2020 surface area analyzer (Fig. 2.3). The samples were de-gasified at 120 °C for 2 h earlier than the BET measurements to remove any adsorbed gases.



**Fig. 2.3.** BET Surface area analyzer.

### **2.3.3. X-ray powder diffraction studies (XRD)**

It is a swift analytical technique used for the detection of crystal structure and atomic spacing of the sample. In this technique, X-Rays are incident to the sample and the interaction constructs a diffracted ray on satisfying a Bragg's rule ( $n\lambda = 2d \sin \theta$ ). Where,  $n$  is an integer,  $\lambda$  is the wavelength of x-rays,  $d$  is the inter-planar spacing in the specimen and  $\theta$  is the diffraction angle. This law reveals the correlation between the wavelength of electromagnetic radiation and the diffraction angle along with lattice spacing in the material. Translation of diffraction peaks into d-spacing one can be aware of the element as each element possesses set of distinctive d-spacing. XRD patterns were recorded on Bruker AXS D8 Advance X-ray powder diffractometer (Fig. 2.4) with a  $\text{CuK}\alpha$  ( $\lambda=1.54058$ ) target and movable detector, which scans the intensity of diffracted radiation within the range of  $5^\circ$ – $60^\circ$  as a function of the angle  $2\theta$  between the incident and diffracted beams. This beneficial analysis was performed for graphite, GO, A-*f*-GO, Cl-*f*-GO and all catalysts to check the crystallinity of the material whether remains intact or not on grafting of metal complexes.

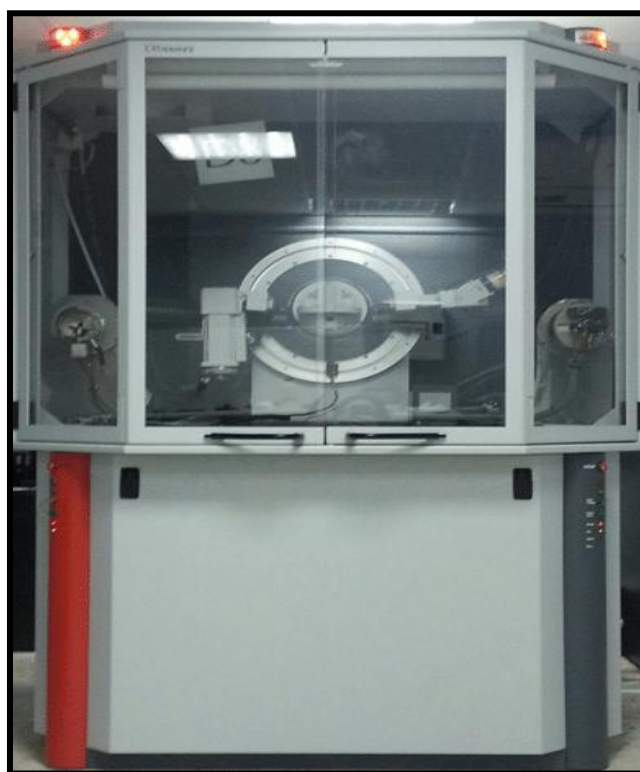


**Fig. 2.4.** X-ray diffractometer.

#### 2.3.4. Fourier-transform infrared (FTIR) spectroscopy

It is well adaptable and appreciative spectrochemical imaging tool to analyze the spatial arrangement of the component sample. FTIR (4000–400  $\text{cm}^{-1}$ ) of the as-prepared catalysts was record with KBr pellets on a model FTIR8400S Shimadzu (Fig. 2.5). It gives information on the vibrational and rotational modes of motion of a molecule and hence an important technique for identification and characterization of various functional groups, nature of atoms and their linkage present in the compound. FTIR is rapidly becoming the ideal compound testing technology owing to their speed, precision and reliability. However, infrared microscopy provides the highest sensitivity and widest spectral range for small area FTIR measurements, collecting microscopic chemical picture of your sample can be time consuming, depending on the data collection and sample size requirements.

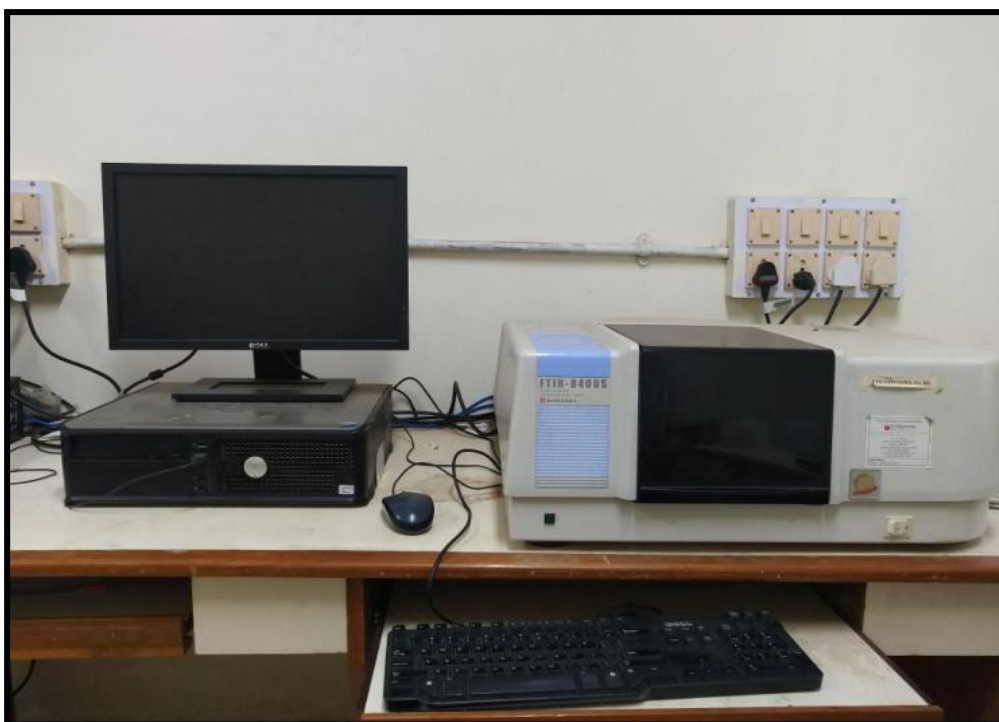


**Fig. 2.5.** FTIR spectrophotometer.

#### 2.3.5. Raman spectroscopy

It is a spectroscopic technique typically used to determine vibrational modes of molecules and to endow with a structural fingerprint which is very helpful in the identification of the molecules. In Raman spectroscopy, a

monochromatic laser light is used to interact with molecular vibrational mode and phonons which results into the energy with laser photons and shifted up (anti-Stokes) or down (Stokes) through elastic scattering.

However, it is being more constructive by recognizing vibrational mode only using laser light to characterize particularly carbonaceous materials. In this research work, we have performed Raman analysis of GO, A-*f*-GO, Cl-*f*-GO and all synthesized catalysts was performed to substantiate the successful synthesis and functionalization by measuring the degree of disorder and ID/IG ratio. Raman spectra of the samples were performed with Technos Raman spectrometer using 532 nm DPPS laser (Laser Quantum Gem 100 mW) 785 nm DPPS Laser (Integrated Optical Match Box 500 mW), Peltier cooled CCD detector (Fig. 2.6).



**Fig. 2.6.** Raman Spectrometer.

### **2.3.6. Electronic spectra**

It is also known as absorbance or reflectance spectroscopy in part of the ultraviolet and full visible regions. It utilizes the light in the UV/Vis. range and affects the color of the material. By absorbing the energy in this region, molecule experiences electronic transitions to higher anti-bonding molecular orbitals. Electrons which can easily get excited absorbed the longer wavelength of the light. Mainly four types of transitions are likely to happen in the order of:  $\sigma \rightarrow \sigma^* > n \rightarrow \sigma^* > \pi \rightarrow \pi^* > n \rightarrow \pi^*$ . This analytical technique is

used for the quantitative determination of the analytes and highly conjugated organic compounds. Electronic spectra of GO, A-*f*-GO, Cl-*f*-GO all synthesized catalysts were recorded on UV-2450 spectrophotometer (200-800 nm) from Shimadzu (Fig. 2.7) using a quartz cell of 1 cm<sup>3</sup> optical path.



**Fig. 2.7.** UV/Vis Spectrophotometer.

### **2.3.7. Thermogravimetric analysis (TGA)**

It is a method of thermal analysis in which changes in physical and chemical properties of samples are measured as a function of increasing temperature with constant heating rate or as a function of time. It deals with the changes in the mass of a material over a period of time as the temperature changes or increases. This analytical technique is very useful in determining the thermal stability of any material. For this research work, thermogravimetric analysis was recorded over Shimadzu TGA50 (Fig. 2.8) in the temperature range of 40 to 700 °C at 10 °C min<sup>-1</sup> in air ambience; the water content was calculated from the weight loss from room temperature to 100 °C.



**Fig. 2.8.** Thermogravimetric instrument.

### **2.3.8. Transmission electron microscopy (TEM)**

It is the most vital tool to characterize the nanomaterials in terms of size of the particles, size distribution and surface morphology. In this analytical technique, a high energy beam of electrons due to much smaller wavelength than light is passing through a thin film of the sample. By the interaction between incident electron beam and the atoms, TEM images are formed and one can examine the crystal structure, surface morphology, growth of layers, high resolution can give information about the shape, size and density of the quantum dots in the materials. TEM analyses of the synthesized samples were performed on a Philips, Tecnai 20 transmission electron microscope (Fig. 2.9). The samples were prepared by placing a drop of primary sample on a porous carbon copper grid and drying in an oven.

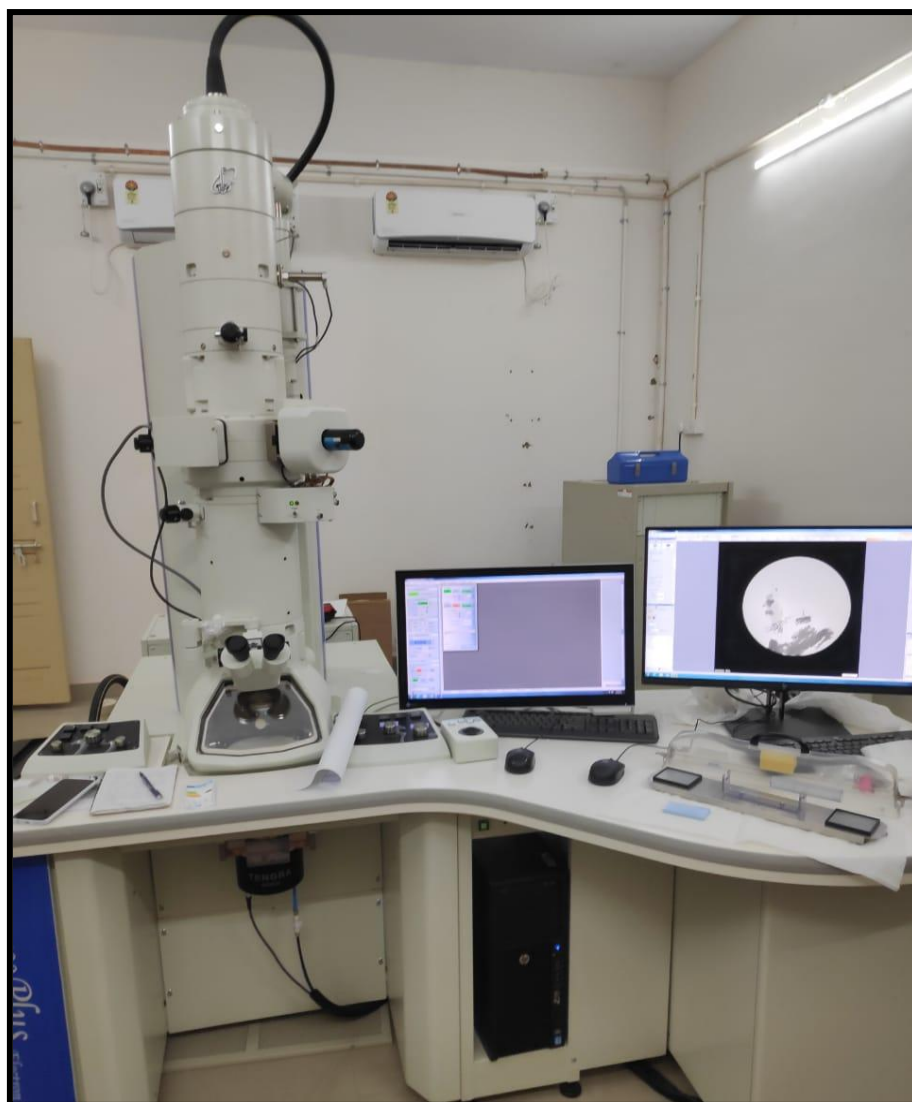


**Fig. 2.9.** Transmission electron microscope.

### **2.3.9. X-ray photoelectron spectroscopy (XPS)**

It is also known as surface sensitive quantitative technique which assesses the elemental composition, empirical formula, chemical state and electronic state of the elements within a material. It is most powerful technique as it not only detect all the elements with atomic number 3 and above but also give the most significant information about the bonding environment of the elements present in the molecule. XPS is routinely used to analyze inorganic compounds, metal alloys, semiconductors, polymers, elements, catalysts, glasses, ceramics, paints, papers, inks, woods, plant parts, make-up, teeth, bones, medical implants, bio-materials, viscous oils, glues, ion-modified materials and many others.

By computing the kinetic energy of the emitted electrons, one can determine the surface nearer element, its chemical states and the binding energy of the electron. The binding energy depends upon a number of factors, which include:

- The kind of element from which the electron is emitted.
- The orbital from which the electron is ejected.
- The chemical environment of the atom.

XPS spectra of the synthesized samples were measured on Specs, Phoibios 225 spectrometer (Fig. 2.10) with Al K $\alpha$  radiation (1486.6 eV).



**Fig. 2.10.** X-ray photoelectron spectroscope.

## 2.4. References

1. S. Rasalingam, R. Peng and R. T. Koodali, *Nanomaterials*, 2014, **2014**, 1-42.
2. R. Thapa, S. Maiti, T. H. Rana, U. N. Maiti and K. K. Chattopadhyay, *J. Mol. Catal. A Chem.*, 2012, **363**, 223-229.
3. Z. Guo, R. Ma and G. Li, *Chem. Eng. J.*, 2006, **119(1)**, 55-59.
4. J. Yang, C. Chen, H. Ji, W. Ma and J. Zhao, *J. Phys. Chem. B*, 2005, **109(46)**, 21900-21907.
5. I. K. M. Yu , D. C. W. Tsang , A. C. K. Yip , S. S. Chen , Y. S. Ok and C. S. Poon, *Bioresour. Technol.*, 2016, **219**, 338-347.
6. J. R. Ludwig and C. S. Schindler, *Catalyst: Sustainable Catalysis. Chem*, 2017, **2(3)**, 313-316.
7. L. de Martin, A. Fabre and J. R. van Ommen, *Chem. Eng. Sci.*, 2014, **112**, 79-86.
8. A. A. Esmailpour, R. Zarghami and N. Mostoufi, Proceedings of the 2015 International Conference on Modeling, Simulation and Applied Mathematics, Atlantis Press, 2015. ISBN: 978-94-6252-104-9. <https://doi.org/10.2991/msam-15.2015.55>.
9. J. Chaouki, C. Chavarie and D. Klvana, *Powder Technol.*, 1985, **43**, 117-125.
10. S. Morooka, K. Kusakabe, A. Kobata and Y. Kato, *J. Chem. Eng. Jpn.*, 1988, **21**, 41-46.
11. A. D. McNaught and A. Wilkinson, IUPAC. Compendium of Chemical Terminology, 2nd ed. (the "Gold Book"), Blackwell Scientific Publications, Oxford, 1997. ISBN: 0-9678550-9-8. <https://doi.org/10.1351/goldbook>.
12. M. P. McDaniel, 'A review of the Phillips supported chromium catalyst and its commercial use for ethylene polymerization' in B. C. Gates, H. Knözinger, *Advances in Catalysis*, Elsevier, Chap-3, 2010, **53**, pp. 123-606.
13. K. Foger, 'Dispersed Metal Catalysts' in J. R. Anderson and M. Boudart, *Catalysis-science and technology*, Springer-Verlag, Berlin, Chap-4, 1984, **6**, 227-305.

14. J. F. Le Page, J. Limido, E. B. Miller and R. L. Miller, *Applied Heterogeneous Catalysis: Design-Manufacture-Use of Solid Catalysts*. Paris Éditions Technip, 1987.
15. C. Perego and P. Villa, *Catal. Today*, 1997, **34**, 281-305.
16. G. J. Hutchings and J. C. Vedrine, 'Catalyst preparation' in M. Baerns, *Basic principles in applied catalysis*, Springer series in chemical physics, Springer, Berlin, Heidelberg, 2004, **75**.
17. J. R. Regalbuto, *Catalyst preparation science and engineering*, CRC Press: Boca Raton, FL, USA. 2007. ISBN-13: 978-0-8493-7088-5.
18. Y. Sakata, Y. Tamaura, H. Imamura, M. Watanabe, *Scientific bases for the preparation of heterogeneous catalysts*, 2006, 331-338.
19. A. N. Akin, M. Ataman, A. E. Aksoylu and Z. I. Oensan, *React. Kinet. Catal. Lett.*, 2002, **76(2)**, 265-270.
20. R. Parthasarathy and S. Spring, US Pat. 3933883, 1976, to W. R. Grace & Co.
21. M. Nawardali and D. Bianchi, *Appl. Catal. A Gen.*, 2002, **231(1-2)**, 45-54.
22. B. Botti, D. Cauzzi, P. Moggi, G. Predieri and R. Zanoni, *Stud. Surf. Sci. Catal.*, 2000, **130B**, (International Congress on Catalysis, 2000, Pt. B), 1091.
23. X. Fan, G. Zhang and F. Zhang, *Chem. Soc. Rev.*, 2015, **44**, 3023-3035.
24. S. Park and R. S. Ruoff, *Nat Nanotechnol.* 2009, **4(4)**, 217-224.
25. H. He and C. Gao, *ACS Appl. Mater. Interfaces*, 2010, **211**, 3201-3210.
26. M. D. Stoller, S. J. Park, Y. W. Zhu and R. S. Ruoff, *Nano Lett.*, 2008, **8**, 3498-3502.
27. J. K. Nam, M. J. Choi, D. H. Cho, J. K. Suh and S. B. Kim, *J. Mol. Catal. A Chem.*, 2013, **370**, 7-13.
28. M. C. Hsiao, S. H. Liao, M. Y. Yen, P. I. Liu, N. W. Pu, C. A. Wang and C. C. Ma, *ACS Appl. Mater. Interfaces.*, 2010, **2(11)**, 3092-4000.
29. O. Akhavan, *ACS Nano*, 2010, **4(7)**, 4174-4180.
30. B. C. Brodie, *Philos. Trans. R. Soc. London*, 1859, **149**, 249-259.
31. W. S. Hummers and R. E. Offeman, *J. Am. Chem. Soc.*, 1958, **80**, 1339-1339.
32. T. Nakajima and Y. Matsuo, *Carbon*, 1994, **32**, 469-475.

33. K. S. Novoselov, D. Jiang, F. Schedin, T. J. Booth, V. V. Khotkevich, S. V. Morozov, and A. K. Geim, *Proc. Natl. Acad. Sci. U.S.A.* 2005, **102**, 10451-10453.
34. A. D. Lueking, L. Pan, D. L. Narayanan and C. E. B. J. Clifford, *Phys. Chem. B*, 2005, **109**, 12710-12717.
35. Y. Matsuo, S. Higashika, K. Kimura, Y. Mayamoto, T. Fukutsuka and Y. J. Sugie, *Mater. Chem.*, 2002, **12**, 1592-1596.
36. H. C. Schniepp J. L. Li, M. J. McAllister, H. Sai, M. H. Alonso, D. H. Adamson, R. K. Prud'homme, R. Car, D. A. Saville and I. A. Aksay, *J. Phys. Chem. B*, 2006, **110**, 8535-8539.
37. J. L. Li, K. N. Kudin, M. J. McAllister, R. K. Prud'homme, I. A. Aksay and R. Car, *PRL*, 2006, **96**, 176101-4.
38. A. Bagri, C. Mattevi, M. Acik, Y. J. Chabal, M. Chhowalla and V. B. Shenoy, *Nat. Chem.*, 2010, **2(7)**, 581-587.
39. J. T. Paci, T. Belytschko and G. C. Schatz, *J. Phys. Chem. C*, 2007, **111(49)**, 18099-18111.
40. R. Kou, Y. Shao, D. Mei, Z. Nie, D. Wang, C. Wang, V. V. Viswanathan, S. Park, I. A. Aksay, Y. Lin, Y. Wang and J. Liu, *J. Am. Chem. Soc.*, 2011, **133**, 2541-2547.
41. H. Vedala, D. C. Sorescu, G. P. Kotchey and A. Star, *Nano Letters*, 2011, **6**, 2342-2347.
42. D. W. Boukhvalov and M. I. Katsnelson, *Nano Lett.*, 2008, **8**, 4373-4379.
43. Z. Li, S. Wu, H. Ding, D. Zheng, J. Hu, X. Wang, Q. Huo, J. Guan and Q. Kan, *New J. Chem.*, 2013, **37(5)**, 1561-1568.
44. Q. Zhao, C. Bai, W. Zhang, Y. Li, G. Zhang, F. Zhang and X. Fan, *Ind. Eng. Chem. Res.*, 2014, **53**, 4232-4238.
45. A. Kumar, S. Layek, B. Agrahari, S. Kujur and D. D. Pathak, *ChemistrySelect*, 2019, **4**, 1337-1345.
46. S. Niyogi, E. Bekyarova, M. E. Itkis, J. L. McWilliams, M. A. Hamon and R. C. Haddon, *J. Am. Chem. Soc.*, 2006, **128**, 7720-7721.
47. Y. Xu, Z. Liu, X. Zhang, Y. Wang, J. Tian, Y. Huang, Y. Ma, X. Zhang and Y. Chen, *Adv. Mater.*, 2009, **21**, 1275-1279.
48. Z. B. Liu, Y. F. Xu, X. Y. Zhang, X. L. Zhang, Y. S. Chen and J. G. Tian, *J. Phys. Chem. B*, 2009, **113**, 9681-9686.

49. X. Zhang, Y. Huang, Y. Wang, Y. Ma, Z. Liu and Y. Chen, *Carbon*, 2009, **47**, 334-337.
50. R. I. Kureshy, N. H. Khan, S. H. R. Abdi, S. T. Patel and P. Iyer, *J. Mol. Catal. A Chem.*, 1999, **150(1-2)**, 175-183.
51. Y. K. Aoyama, T. Fujisawa, T. Walanabe, H. Toi and H. Ogashi, *J. Am. Chem. Soc.*, 1986, **108(5)**, 943-947.
52. T. R. Kelly, A. Whiting and N. S. Chandrakumar, *J. Am. Chem. Soc.*, 1986, **108(12)**, 3510-3512.
53. B. Paulchamy, G. Arthi and B. D. Lignesh, *J. Nanomed. Nanotechnol.*, 2015, **6(1)**, 1-4.